Inorganic Chemistry

pubs.acs.org/IC

Article

Insights into the Mechanism of CO_2 Electroreduction by Molecular Palladium−Pyridinophane Complexes

Sagnik Chakrabarti, Toby J. Woods, and Liviu M. Mirica*

Cite This: *Inorg. Chem.* 2023, 62, 16801−16809

Read Online

ACCESS | Metrics & More | Article Recommendations | Supporting Information

ABSTRACT: Herein, we report the synthesis, characterization, and electrocatalytic CO_2 reduction activity of a series of Pd(II) complexes supported by tetradentate pyridinophane ligands. In particular, we focus on the electrocatalytic CO_2 reduction activity of a Pd(II) complex supported by the mixed hard−−soft donor ligand 2,11-dithia[3.3](2,6)-pyridinophane (N2S2). We also provide spectroscopic evidence of a CO-induced decomposition pathway for the same catalyst, which provides insights into catalyst poisoning for molecular Pd CO_2 reduction electrocatalysts.

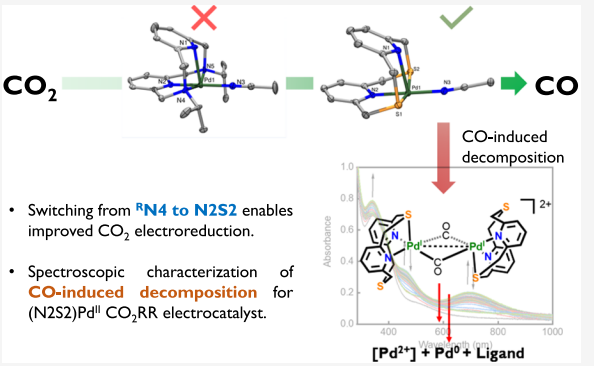

INTRODUCTION

There has been steadily growing interest in studying well-defined molecular complexes for performing CO_2 reduction over the past four decades. Significant effort has been directed toward the development of molecular electrocatalysts for reducing CO_2 to CO.[1,2] Product selectivity and the ability to rationally design ligands to improve activity have been key reasons for the extensive efforts put into studying the mechanism of molecular electrocatalysts. Key classes of compounds that have been shown to be efficient for reducing CO_2 to CO are, among others, metalophthalocyanines,[3,4] metaloporphyrins,[4−6] polypyridyl rhenium and manganese carbonyls,[7] nickel complexes with azamacrocyclic ligands,[8] and polypyridyl complexes of Co/Fe/Ni.[9] The development of another class of molecular electrocatalysts, Pd-triphosphines (Scheme 1a), was led by the DuBois group for over 15 years.[10] These pincer complexes had the general formula $[Pd(L_3)(CH_3CN)]^{2+}$ and were shown to be efficient catalysts for the reduction of CO_2 to CO in $[DMF\text{-}H]^+$ and CH_3CN.[11−13] Extensive mechanistic studies revealed that the formation of Pd(I)−Pd(I) dimers resulted in low rates and turnover numbers (TONs). A bimetallic version of the complex was shown to be a very fast catalyst, albeit with low turnovers.[14] More recently, the Wolf group reported several new bis-N-heterocyclic carbene (bis-NHC)-based pincer complexes with Pd for CO_2 reduction (Scheme 1a), with low Faradaic efficiencies (FEs).[15−17] A palladium complex with a mixed aza-thioether macrocyclic ligand was recently reported by Yang and co-workers (Scheme 1a),[18] and they showed that using suitable proximal cations in a synthetically appended azacrown ether can suppress the competing hydrogen evolution reaction (HER), with a modest improvement in the selectivity for CO_2 reduction to CO, although Faradaic efficiencies for CO remained very low (<10%).

We have recently reported that nickel complexes supported by thiapyridinophane ligands can catalyze electrochemical hydrogen evolution by $Ni^{0/II}$ or $Ni^{I/III}$ cycles.[19,20] In this study, we report three key findings.[21] First, Pd complexes supported by azamacrocyclic pyridinophane ^{R}N4 ligands (Scheme 1b, entries 2−4) are inefficient catalysts for CO_2 reduction as they are prone to rapid decomposition during electrolysis. Second, on switching to a mixed hard/soft donor atom thiapyridinophane N2S2 ligand, which has been used previously to stabilize Pd(I) species,[22] the CO_2 reduction activity of the complex (Scheme 1b, entry 1) is enhanced considerably. Third, a decomposition route was identified for the catalyst that involves the reduction of Pd^{II} by CO and H_2O, offering insights into catalyst poisoning and the general inefficiency of previously reported molecular Pd complexes for CO_2 reduction. It represents a modest improvement in stability and catalytic performance over other recently reported palladium complexes, which contain mixed hard/soft donor atoms.[15−18]

Received: July 4, 2023
Published: October 3, 2023

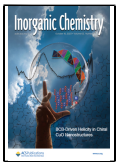

https://doi.org/10.1021/acs.inorgchem.3c02236
Inorg. Chem. 2023, 62, 16801−16809

Scheme 1. (a) Reported Molecular Palladium Complexes for Electrochemical CO_2 Reduction from the DuBois, Wolf, and Yang Groups; (b) Molecular Structures of the Palladium−Pyridinophane Complexes Discussed in This Study

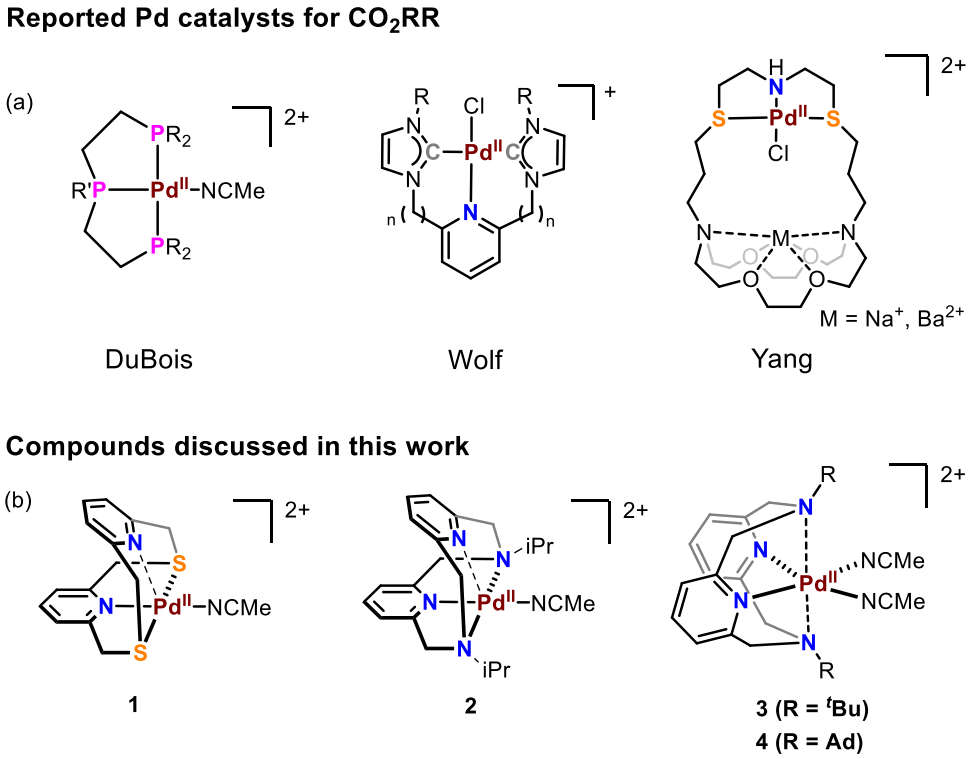

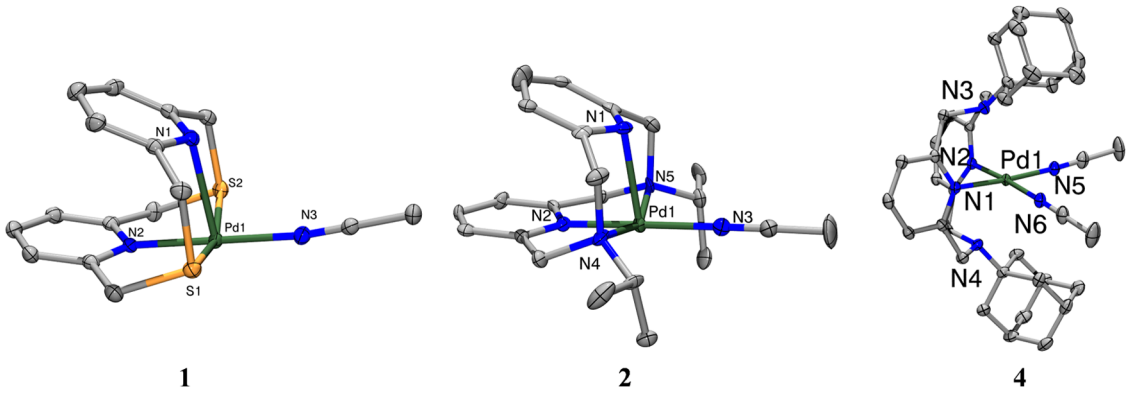

Figure 1. Oak Ridge thermal ellipsoid plot (ORTEP) representations of the dications of **1**, **2**, and **4**, shown with 50% thermal ellipsoids and with the counteranions and H atoms omitted for clarity. Selected bond distances for (in Å) **1**: Pd1−N1: 2.529(2); Pd1−S1: 2.3286(8); Pd1−S2: 2.3429(8); Pd1−N2: 2.008(2); Pd1−N3: 1.999(3), **2**: Pd1−N1: 2.419(18); Pd1−N2: 1.939(18); Pd1−N3: 2.014(21); Pd1−N4: 2.145(24); Pd1−N5: 2.159(24) and **4**: Pd1−N1/N2: 2.0198(17); Pd1−N3/N4: 2.623(1); Pd1−N5/N6: 2.0276(18).

RESULTS AND DISCUSSION

Synthesis and Characterization of Compounds 1−4. The synthesis of all of the ligands used in this study has been reported previously.[23−26] The general protocol for synthesizing the complexes is as follows: a dichloromethane solution of the ligand was added to an acetonitrile solution of $[Pd(MeCN)_4][BF_4]_2$, which resulted in a color change from yellow to reddish-brown [(N2S2), **1**], dark brown (^{iPr}N4, **2**), or dark green (for ^{tBu}N4, **3** and ^{Ad}N4, **4**). The crystal structures for **1**[23] and **3**[27] have been reported previously. **1**, previously crystallized as a dinuclear complex with a $Pd^{II}−Pd^{II}$ interaction,[23] was crystallized herein as a mononuclear species (Figure 1). The newly synthesized complexes **2** and **4** have been characterized by UV−vis, NMR, EA, electrospray ionization mass spectrometry (ESI-MS), and single-crystal X-ray diffraction. While all four compounds adopt formally square planar geometries, the bond parameters suggest that **1** and **2** are better described as distorted square pyramidal around the Pd, while **3** and **4** adopt a tetragonally distorted octahedral geometry. The Pd1−N1 bond distances are 2.529 Å in **1** and 2.416 Å in **2**, suggestive of significant electrostatic interactions between the Pd^{II} center and the nitrogen lone pair on pyridine. The equatorial planes of the Pd^{II} centers in **2** and **3** are defined by a pyridine nitrogen, the two amine or thioether arms, and an acetonitrile molecule. By comparison, the Pd^{II} complexes of the ^{tBu}N4 and ^{Ad}N4 ligands, which have similar steric profiles, adopt a distorted octahedral geometry, where the equatorial plane is defined by pyridine N atoms ($Pd−N_{py}$ average distance of 2.02 Å for **3**[27] and **4**) and the nitrogen from the solvent (2.01 Å for **3**[27] and 2.02 Å for **4**).

https://doi.org/10.1021/acs.inorgchem.3c02236
Inorg. Chem. 2023, 62, 16801−16809

Electrochemical CO_2 Reduction with 2−4. Our initial studies focused on the electrochemical reduction of CO_2 with the ^{R}N4 palladium complexes **2**−**4**. The cathodic region of the voltammograms is in general complicated to interpret and features several irreversible peaks (Figure 2). This is in accordance with previously reported pyridinophane complexes, which have different conformations in solution, which lead to different reduction potentials.[27,28] For **2**, the E_{pc1} (cathodic peak potential for the first reduction) is at −0.64 V versus $Fc^{+/0}$. It is interesting to note that this event, which likely corresponds to a $Pd^{II/I}$ reduction, is cathodically shifted for **3** and **4**, when compared to **2**. This can be rationalized by the more electron-donating nature of the *t*Bu and Ad substituents in **3** and **4**, respectively, compared to *i*Pr in **2**.

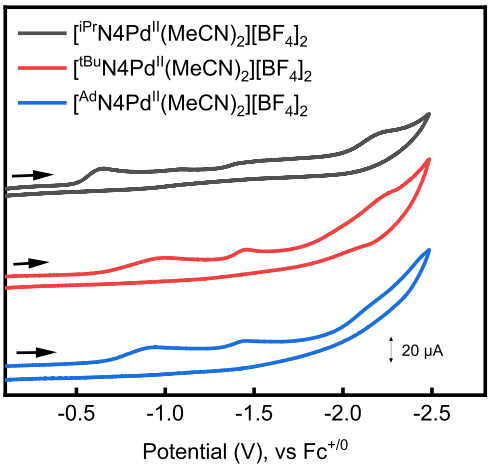

Figure 2. Comparative cyclic voltammograms (CVs) of $[(^{R}N4)Pd^{II}(MeCN)_2]^{2+}$ compounds recorded under N_2 in 1 mM solutions of **2** (black trace), **3** (red trace), and **4** (blue trace) in a 0.1 M $TBAPF_6$/MeCN solution. The arrow represents the direction of the scan.

We found that the CVs indicate that CO_2 binds at **2** (Figure S11) and that titrating weak acids (2,2,2-trifluoroethanol (TFE) and phenol) leads to catalytic currents (Figure S15). Background CVs with acids only (Figure S14) revealed that the hydrogen evolution window is distinct from the CO_2 reduction window when TFE was used as the acid. However, we found that the catalyst decomposes rapidly under bulk electrolysis conditions with an exponential increase in the current density versus time (Figure S16). No gases were detected in gas chromatography-mass spectrometry (GC-MS), and no soluble products were detected by NMR spectroscopy. Since Dubois and co-workers found that using bulkier ligands to prevent the formation of Pd^{I} dimers for Pd−phosphine complexes was detrimental to CO_2 reduction, we tested the bulkier analogues **3** and **4** for CO_2 reduction. However, similar issues with catalyst decomposition were observed, suggesting that Pd complexes with ligands containing hard N-donors are unsuitable for electrochemical CO_2 reduction (pages S13−S17). Noting this, we hypothesized that switching to soft

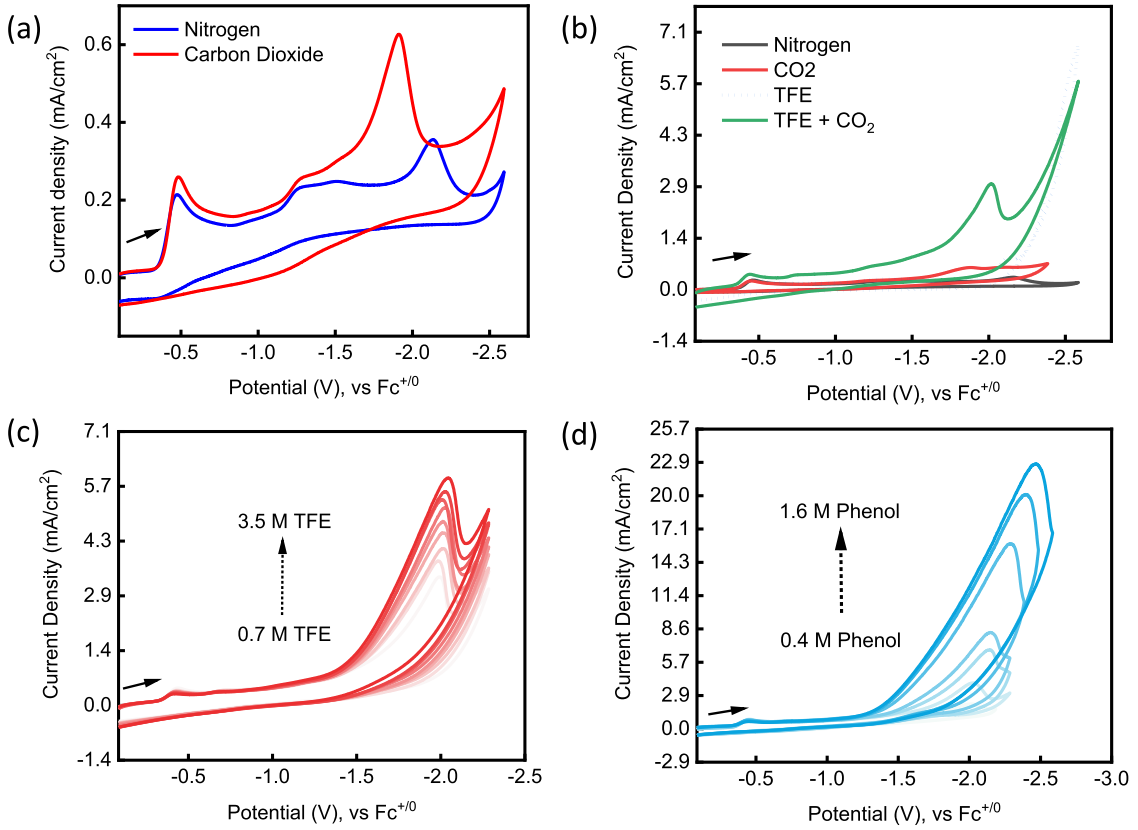

Figure 3. (a) Cyclic voltammograms of **1** under N_2 (blue) and CO_2 (red) saturation; (b) cyclic voltammograms of **1** under N_2 (black), CO_2 (red), 0.7 M TFE (dotted blue), and 0.7 M TFE + CO_2 (green), showing the different windows of hydrogen evolution and CO_2 reduction in the presence of **1**; (c) TFE titrations into a CO_2-saturated 0.1 M $TBAPF_6$/MeCN solution of **1** (1 mM); and (d) phenol titrations into a CO_2-saturated MeCN/0.1 M $TBAPF_6$ solution of **1** (1 mM). The bold arrows represent the direction of the scan. The dotted arrows represent the increasing amounts of acid titrated into the MeCN solution containing **1**.

https://doi.org/10.1021/acs.inorgchem.3c02236
Inorg. Chem. 2023, 62, 16801−16809

Scheme 2. Proposed Mechanism of CO_2 Electroreduction with 1 Following a Generalized EECC Mechanism, and the Pathway of Decomposition of 1 in the Presence of CO[a]

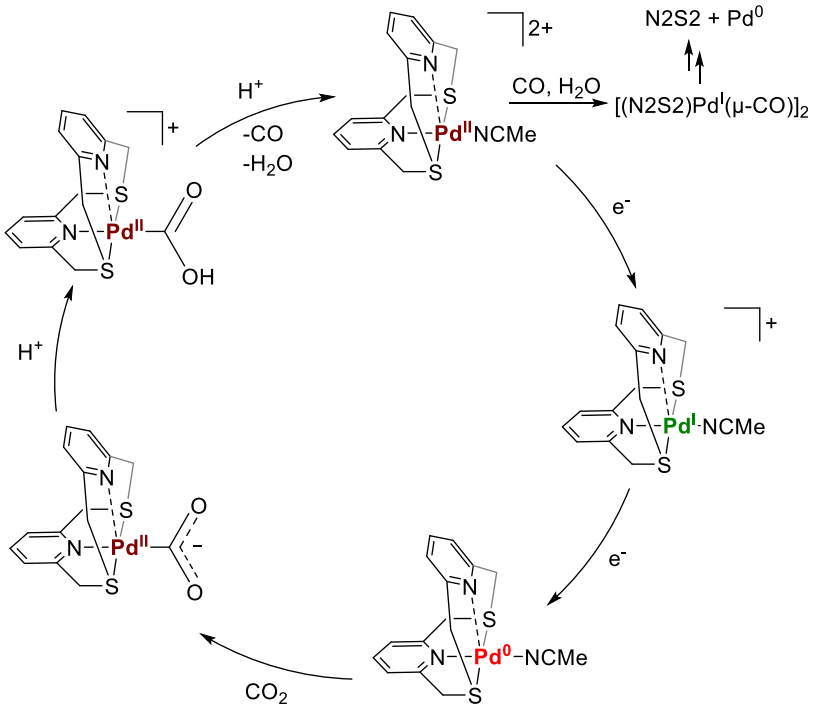

[a]The decomposition of 1 by CO is also included in the mechanism, which is described in the subsequent section.

donors in the same pyridinophane framework may aid in stabilizing low-valent states and lead to improved CO_2 electroreduction.

Electrochemical CO_2 Reduction with 1. The CVs of **1** recorded under a N_2 atmosphere showed two distinct irreversible faradic processes. The first reduction (E_{pc1} = −0.49 V versus $Fc^{+/0}$, Figure 3a) was assigned to a $Pd^{II/I}$ process, which is anodically shifted compared to the ^{R}N4 analogues, indicating that the soft thioether ligands can better stabilize Pd^{I}. The second reduction (E_{pc2}, the cathodic peak potential for the second reduction = −2.1 V versus $Fc^{+/0}$, Figure 3a) was assigned to a $Pd^{I/0}$ process. The slope of the plot of i_{pc} (peak cathodic current) versus the square root of the scan rate is linear for both of these cathodic processes, suggestive of a homogeneous behavior in solution (Figure S20).[29] The slopes of peak shift versus the logarithm of scan rate were 43 and 53 mV/dec, respectively (Figure S21), which are large deviations from the theoretically predicted slope of 29 mV/dec for an ideal Nernstian EC process.[29] The irreversibility in the faradic processes seen in the CV was assigned to electron transfers, followed by structural changes on reduction (ligand dissociation and/or conformational changes), as has been observed previously for related Pd pyridinophane complexes.[27] The CVs of **1** in a CO_2-saturated solution showed a cathodic feature at −1.92 V versus $Fc^{+/0}$ (Figure 3a). This peak showed an approximate 2-fold enhancement in peak current, even in the absence of any Brønsted or Lewis acids, which may be due to the electrochemical disproportionation of CO_2 to CO and CO_3^{2-}, as seen in Ru polypyridyl complexes.[1] An anodic shift of 220 mV with respect to E_{pc2} was seen, which is consistent with CO_2 binding at the Pd center. Furthermore, there is no change in E_{pc1}, suggesting that CO_2 reacts with Pd^{0} and not Pd^{I}. In order to examine the activity of **1** toward electrocatalytic CO_2 reduction, we titrated 2,2,2-trifluoroethanol (TFE) (Figure 3c) and phenol (Figure 3d) into CO_2-saturated MeCN solutions of **1**. Scan rate-independent current densities were obtained with 3.5 M TFE (Figure S25) and 1.6 M phenol (Figure S24). From these experiments, k_{obs} was calculated to be 4496 s^{-1} when phenol was used as a proton source and 423 s^{-1} when TFE was used as a proton source (page S22). Control experiments in the presence of acids suggest only limited background contribution from glassy carbon (Figure S22) and an insignificant rate of proton reduction in the potential window under consideration (Figure 3b). Following the method of Appel and Helm,[30] we calculated the overpotential of CO_2 reduction (at the potential corresponding to half of the peak catalytic current density, $E_{cat/2}$) to be 230 mV (Figure S25) when using a 1:1 PhOH/NaOPh buffer (pK_a in acetonitrile = 29) as a proton source. However, we did see CO when performing electrolysis with phenol at −2 V (29% FE, Table S3), indicating that CO is produced at overpotentials as low as 160 mV. A higher overpotential of 370 mV is obtained if a pK_a of 35.4 is considered for TFE in acetonitrile. These observations suggest that a normal rate-overpotential scaling relationship is followed for **1**, i.e., CO_2 reduction with weaker acids has sluggish kinetics but operates at a lower overpotential. Upon electrolyzing a CO_2-saturated solution containing 1 mM **1** in the presence of 1 M phenol or 1 M TFE at −2.1 V versus $Fc^{+/0}$, CO was produced, as detected by GC (Figure S38). The Faradaic efficiency (FE) of CO production was determined to be around 70%, and we could not detect the formation of any H_2 by GC or formate in the NMR. This suggests that **1** is a selective electrocatalyst for the reduction of CO_2 to CO. Interestingly, an intense orange color (vide infra) developed as the electrolysis progressed (Figures S33 and S34), and this resulting solution was also active for CO_2 reduction, producing CO with an FE of 79% (Table S3). In order to test for the

https://doi.org/10.1021/acs.inorgchem.3c02236
Inorg. Chem. 2023, 62, 16801−16809

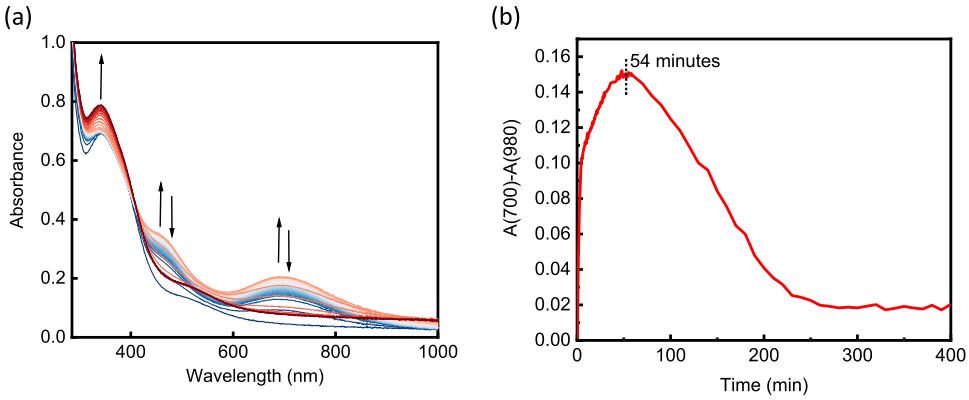

Figure 4. (a) UV−vis spectral changes observed on adding CO to a 1 mM acetonitrile solution of **1**. The spectral changes were recorded for a period of 400 min; the starting spectrum is in dark blue, while the final spectrum is in red. (b) Absorbance versus time profile of the peak at 700 nm. 54 min is marked to indicate the time until which there is a growth in the absorption of the species that forms initially upon the reaction of the Pd^{II} complex with CO. After 54 min, that species gradually dies and forms an unidentified species and Pd black.

homogeneous behavior of **1** in solution, a rinse test was performed, and the lack of Faradaic features in the post-rinse CV indicates that the catalyst is homogeneous in solution (Figure S23). In addition, some CO_2 reduction activity was retained in the presence of a mercury pool (27% FE, Table S3). However, electrolysis over longer periods of time revealed the formation of Pd black and decay in the current versus time profile (Figure S37). Following the method outlined by Savéant et al., we also calculated the turnover frequency (TOF) from electrolysis for 1 h (page S32). A value of 11.8 s^{-1} was found with TFE as the proton source, which is much lower than that calculated from the CVs.

Mechanistic Insights. Preliminary mechanistic studies were performed next, and the linear correlation obtained upon plotting i_{cat} versus the catalyst concentration (Figure S27) and the square root of the acid concentration (Figures S28−S30) indicates that the reaction is first order in the catalyst and acid, respectively. To further probe the role of protons, kinetic isotope effect (KIE) measurements were carried out in the presence of TFE and TFE-d_1. A primary KIE value of 1.5 ± 0.3 (pages S25 and S26) suggests the involvement of a proton in the rate-determining step or in the steps preceding the rate-determining step. This value is in good agreement with the values Kubiak and co-workers reported for the electrocatalytic CO_2 reduction reaction (CO_2RR) with Re-carbonyl complexes using TFE as a proton source.[31] The previously reported palladium catalysts required fairly strong acids for reducing CO_2 to CO. Examples include HBF_4 (pK_a in MeCN = 1.6)[11−13] for the Pd−phosphine complexes and trifluoroacetic acid (TFA) for the Pd−NHC pincer complexes (pK_a in MeCN = 12.7).[15−17] It is interesting to note in this context that **1** reduces CO_2 to CO in the presence of weak acids.[1] Based on these results, we propose that the CO_2 binding equilibrium likely involves a two-electron transfer from the doubly reduced Pd^0 state. This can then react with CO_2 to form a putative Pd^{II}−CO_2^- species that would be extremely basic and can be protonated by weak acids in solution. Thus, we propose that activation of CO_2 by the highly reduced Pd^0 species is the reason electrocatalysis happens even with weak acids.

Involvement of a proton in the rate-determining step indicates that one of the subsequent steps can be rate-determining: (a) the formation of a Pd−COOH intermediate, which involves the protonation of Pd^{II}−CO_2^-; (b) the protonation of the Pd−COOH intermediate to cleave the C−O bond; or (c) the cleavage of the Pd−C bond in a Pd^{II}CO species. Literature evidence shows that for highly reduced species, the reaction between the metal center and CO_2 is extremely fast, as seen in the Fe^0 state of iron porphyrins for CO_2 reduction to CO,[5] and thus, CO_2 binding is likely not rate-determining. Based on these observations and literature precedence, a preliminary mechanism is proposed, as shown in Scheme 2.

Investigation of CO-Induced Decomposition of 1. The instability of **1** during long-term electrolysis and the generally poor performance of molecular palladium catalysts toward CO_2 electroreduction prompted us to investigate possible decomposition pathways for this catalyst. We hypothesized that any insights into this process should be broadly applicable to Pd complexes for CO_2 reduction in general, as all reported complexes have soft donor atoms. The ease of reduction of Pd^{II} to metallic Pd by CO is well-documented in Pd-catalyzed carbonylation chemistry. In this context, a study by Casati et al.[32] reported phenanthroline-supported $[Pd^I(\eta^2\text{-CO})]_2$ dinuclear species as viable decomposition intermediates to metallic Pd and the free ligand. However, we did not find any study that analyzed the decomposition pathways of Pd molecular electrocatalysts for CO_2 reduction.

We began our investigations by monitoring the reaction between **1** and CO by UV−vis spectroscopy. The reaction progress was monitored over time (Figure 4a), to reveal a growth in peaks at 470 and 700 nm for about an hour (Figure 4b). An intermediate, green-colored species cleanly converts to a new species and Pd black with an isosbestic point at 400 nm and decays in absorbances at 470 and 700 nm (Figure 4b). These observations suggest that a reductive process is operating (vide infra). Control experiments revealed that the byproduct is not the homoleptic Pd^I dinuclear complex $[Pd_2(MeCN)_6][BF_4]_2$ or the species formed when CO is added to this complex (Figure S40). Addition of CO to a solution of **1** and 1 equiv of $CoCp_2$ as a sacrificial electron donor results in the same UV−vis absorption features (Figure S39), which indicates that the green species being formed could be a putative $(N2S2)Pd^I$ carbonyl compound. It is interesting to note that the similarity of the absorption spectra suggests that CO can act as a reductant in this chemistry, as noted by Casati and co-workers for Pd phenanthroline complexes.

https://doi.org/10.1021/acs.inorgchem.3c02236
Inorg. Chem. 2023, 62, 16801−16809

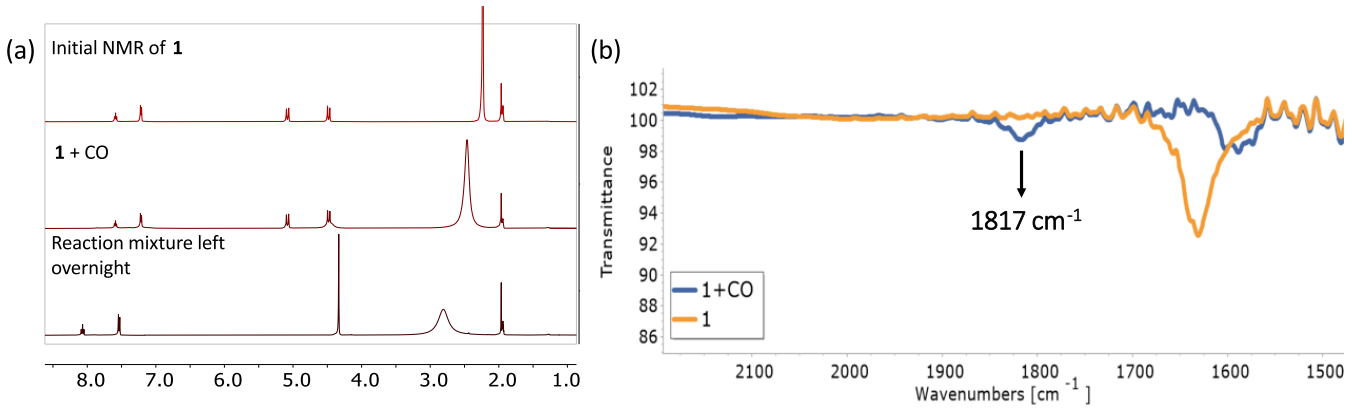

Figure 5. (a) ^{1}H NMR spectroscopic changes observed when CO was added to a CD_3CN solution of **1**. Blue, NMR of **1**; green, 4 min after CO addition; red, NMR of the reaction mixture left overnight. (b) Thin-film IR spectra of **1** (orange) in MeCN, compared to **1** + CO (blue) in MeCN. The solution IR spectrum for **1** + CO has a lower S/N ratio due to formation of Pd^0 black.

Scheme 3. Proposed Decomposition Route of Reacting 1 with CO[a]

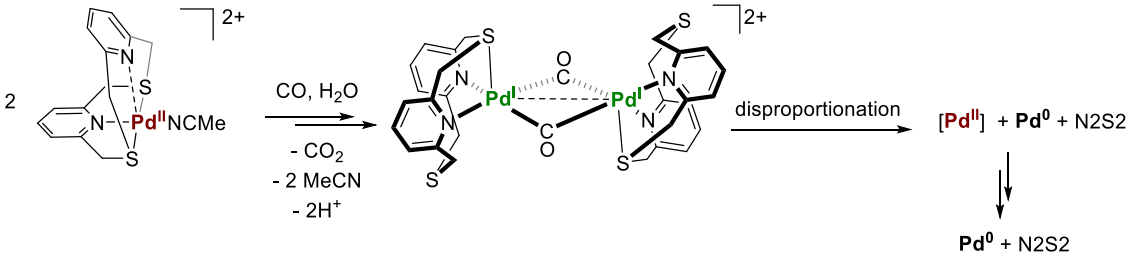

[a]For the first step, CO acts as a reductant to reduce Pd^{II}. For the disproportionation step, the [Pd^{II}] can be **1** or another [(N2S2)Pd^{II}] species.

A similar protocol was followed for the NMR analysis of the reaction, and we recorded the NMR spectra of the complex at various stages of the reaction (Figure 5a). When the integration of the peaks of **1** was compared to that of the peaks of an internal standard (1,3-benzodioxole, pages S35 and S36), a stoichiometric amount of the free ligand formed after 16 h, suggesting a clean conversion into reduced products, which was also confirmed by UV−vis studies. The broadening of the methylene peaks (Figure 5a, middle spectrum and Figure S44) in the NMR of the intermediate species formed upon bubbling CO was reminiscent of a related, structurally characterized isonitrile compound [(N2S2)Pd^I(μ-NC^tBu)]$_2$(ClO_4)$_2$ recently reported by our group.[22] The isoelectronic relationship between CO and *t*BuNC lends further credence to our assignment of the intermediate species as a binuclear Pd^I compound. It is also worth noting that in an earlier report from our group, a transient electron paramagnetic resonance (EPR) signal was generated on reducing **1** with $CoCp_2$.[22] Thus, it is possible that extremely short-lived, unstable mononuclear Pd^I compounds can also potentially be formed in a reductive decomposition pathway.

Finally, the thin-film solution IR spectrum of **1** treated with CO revealed the appearance of a peak at 1817 cm^{-1} (Figure 5b, wider range shown in Figure S46). This is slightly lower than the CO stretch (1873 cm^{-1}, Figure S47) seen when CO is bubbled into [Pd_2(MeCN)$_6$][BF_4]$_2$, indicative of higher back-donation arising from the N2S2 ligand. In addition, a weak IR stretch attributable to CO_2 was seen at 2340 cm^{-1} (Figure S46), which is the expected byproduct of the reduction of **1** by CO. It is worth mentioning that multiple attempts to crystallize the aforementioned binuclear intermediate always resulted in the formation of Pd black, even at lower temperatures, suggesting that it is prone to rapid decomposition.

Based on the results described above, we propose a decomposition route for **1** as shown in Scheme 3, which would explain the instability of the complex toward long-term electrolysis, as buildup of CO in the solution would accelerate the decomposition process. CO, in the presence of H_2O, is the reductant in this chemistry and reduces the Pd^{II} center to Pd^I, with CO_2 being formed as a side product. This is indeed confirmed by the detection of CO_2 in the solution IR when **1** is reacted with CO. The structure of the dinuclear Pd^I species in Scheme 3 is proposed on the basis of the previously reported, structurally characterized [(N2S2)Pd^I(μ-NC^tBu)]$_2$(ClO_4)$_2$ complex.[22] Such a Pd^I species can then undergo disproportionation to form Pd^0 and a Pd^{II} species, and the resulting Pd^{II} species can be further reduced by the excess CO present in the reaction mixture to eventually lead to complete conversion of the initial Pd^{II} complex **1** to Pd^0 black and the free N2S2 ligand. During catalysis, this process is expected to be very slow initially, as only a small amount of CO and H_2O is generated (reflected in the low turnover number). This rationalizes why **1** decomposes when electrolysis is carried out for a longer period of time.

To search for an explanation for the orange color seen during the course of electrolysis (UV−vis spectroscopic changes shown in Figure 6), we considered the direct interaction of **1** with CO_2. Pd complexes supported by bis-NHC or diamine ligands are known that form stable carbonate complexes[33−37] in the presence of CO_2 and water. **1** is unreactive with CO_2 by itself or in the presence of acids (Figure S41). The reaction of **1** with Ag_2CO_3 forms an orange solution, with UV−vis features very similar to that of the

https://doi.org/10.1021/acs.inorgchem.3c02236
Inorg. Chem. 2023, 62, 16801−16809

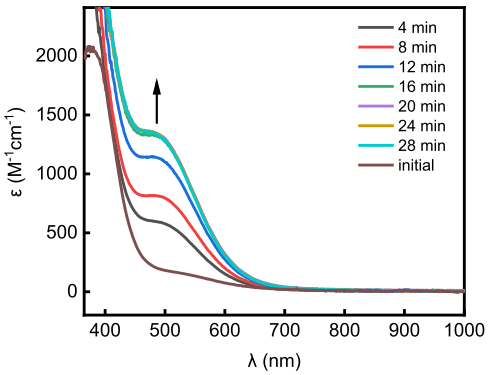

Figure 6. Changes in the UV−vis spectrum of the electrolysis solution containing 1 mM **1** in 0.1 M $TBAPF_6$/MeCN. Aliquots were taken at each given time point from the working electrode chamber, and the UV−vis was recorded.

postelectrolyte solution (Figures S42 and S43). Pd−carbonate complexes are often seen as the end product of protonolysis of Pd−Me complexes in the presence of CO_2 and H_2O.[33] Therefore, we tentatively assign the identity of the orange intermediate seen during electrolysis to a Pd−carbonate complex.

Benchmarking versus Other Pd CO_2RR Catalysts. In order to compare **1** with other palladium electrocatalysts for CO_2RR, we benchmarked its activity against some previously reported complexes (Table 1). While **1** is not comparable to the DuBois triphosphine compounds in terms of long-term stability and Faradaic efficiency for producing CO, it represents an improvement over Pd complexes supported by mixed hard/soft donor atom ligands. In addition, **1** can perform CO_2RR in the presence of weaker acids than HBF_4 or trifluoroacetic acid (TFA), which is likely due to the involvement of the highly reduced Pd^0 state for CO_2 activation.

CONCLUSIONS

In conclusion, we report the electrochemical CO_2 reduction activity of a Pd complex, $[(N2S2)Pd^{II}(MeCN)][BF_4]_2$. This compound displays improved stability and CO_2 reduction activity compared with the structurally related pyridinophane (^{R}N4)Pd complexes, which undergo rapid decomposition under strongly reducing conditions. Additionally, we describe a CO-induced decomposition pathway for **1**, which involves a dinuclear Pd^{I} complex with bridging carbonyl ligands, as suggested by a series of spectroscopic results. We hypothesize that dissociating the CO ligands from the Pd center may improve the activity of these classes of compounds, either by adding a CO scavenger or by photolysis, which is a subject of active research in our group. Overall, we hope that this work will inspire more careful studies into catalyst decomposition in homogeneous electrocatalysts and pave the way for the design of better electrocatalysts with mixed hard/soft donor atoms.

ASSOCIATED CONTENT

Supporting Information

The Supporting Information is available free of charge at https://pubs.acs.org/doi/10.1021/acs.inorgchem.3c02236.

Table 1. Comparison of the Key Catalytic Parameters of 1 versus Literature-Reported Complexes for Which the Values Have Been Reported by the Authors[a]

Catalyst	Conditions	η (V)	log TOF (s^{-1})	FE_{CO} (%)	Ref.
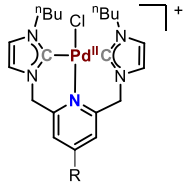	DMF, TFA	0.50 V (half-wave)	0.95 (R=Me) 0.85 (R=H,Br) 0 ($R=CO_2Me$)	25% (R=OMe) 8% (R=H) 10% (R=Br) 0% ($R=CO_2Me$)	15-17
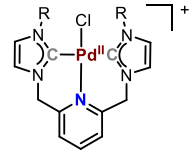 R = cationic residues	DMF, TFA	Not reported	Not reported	Maximum of 49% for one of the reported complexes	15-17
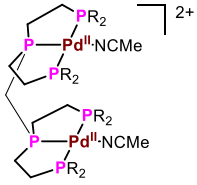	DMF, HBF_4	0.80 V	0.37	99%	14
1	MeCN, TFE/phenol	0.23 V (phenol) 0.37 V (TFE)	1.07	74%	this work

[a]Although other Pd complexes have been reported by Dubois et al., the dinuclear Pd catalyst shown as the third entry is the fastest.[14] For consistency, we report its TOF determined by the method of Savéant et al.[2]

https://doi.org/10.1021/acs.inorgchem.3c02236
Inorg. Chem. 2023, 62, 16801−16809

Detailed experimental details for the improved synthesis of the ligand ^{Ad}N4, synthesis and characterization details (including ^{1}H and ^{13}C NMR spectra, ESI-MS and EA) of the complexes described in this study, homogeneous electrochemical experiments, spectroscopic data for the analysis of the reactions with CO and CO_2 (PDF)

Accession Codes

CCDC 2232617−2232619 contain the supplementary crystallographic data for this paper. These data can be obtained free of charge via www.ccdc.cam.ac.uk/data_request/cif, or by emailing data_request@ccdc.cam.ac.uk, or by contacting The Cambridge Crystallographic Data Centre, 12 Union Road, Cambridge CB2 1EZ, UK; fax: +44 1223 336033.

AUTHOR INFORMATION

Corresponding Author

Liviu M. Mirica − *Department of Chemistry, University of Illinois at Urbana−Champaign, Urbana, Illinois 61801, United States;* orcid.org/0000-0003-0584-9508; Email: mirica@illinois.edu

Authors

Sagnik Chakrabarti − *Department of Chemistry, University of Illinois at Urbana−Champaign, Urbana, Illinois 61801, United States*

Toby J. Woods − *Department of Chemistry, University of Illinois at Urbana−Champaign, Urbana, Illinois 61801, United States;* orcid.org/0000-0002-1737-811X

Complete contact information is available at: https://pubs.acs.org/10.1021/acs.inorgchem.3c02236

Author Contributions

L.M.M. directed the overall project. L.M.M. and S.C. designed the experiments. S.C. performed experimental work. Data analysis was performed by S.C. and L.M.M. S.C. and L.M.M. wrote the manuscript. T.J.W. collected the diffraction data and solved the crystal structure of **2**.

Notes

The authors declare no competing financial interest.

ACKNOWLEDGMENTS

The authors thank the National Science Foundation (CHE-2102544) for financial support, Dr. Bronte Charette (Olshansky lab) for helping with the IR data collection, and the research facilities at the University of Illinois at Urbana−Champaign for assistance.

REFERENCES

(1) Francke, R.; Schille, B.; Roemelt, M. Homogeneously Catalyzed Electroreduction of Carbon Dioxide—Methods, Mechanisms, and Catalysts. *Chem. Rev.* **2018**, *118*, 4631−4701.

(2) Costentin, C.; Robert, M.; Savéant, J.-M. Catalysis of the electrochemical reduction of carbon dioxide. *Chem. Soc. Rev.* **2013**, *42*, 2423−2436.

(3) Wu, Y.; Liang, Y.; Wang, H. Heterogeneous Molecular Catalysts of Metal Phthalocyanines for Electrochemical CO2 Reduction Reactions. *Acc. Chem. Res.* **2021**, *54*, 3149−3159.

(4) Nikoloudakis, E.; López-Duarte, I.; Charalambidis, G.; Ladomenou, K.; Ince, M.; Coutsolelos, A. G. Porphyrins and phthalocyanines as biomimetic tools for photocatalytic H2 production and CO2 reduction. *Chem. Soc. Rev.* **2022**, *51*, 6965−7045.

(5) Costentin, C.; Drouet, S.; Robert, M.; Savéant, J.-M. A Local Proton Source Enhances CO2 Electroreduction to CO by a Molecular Fe Catalyst. *Science* **2012**, *338*, 90−94.

(6) Costentin, C.; Robert, M.; Savéant, J.-M.; Tatin, A. Efficient and selective molecular catalyst for the CO2-to-CO electrochemical conversion in water. *Proc. Natl. Acad. Sci. U.S.A.* **2015**, *112*, 6882−6886.

(7) Grice, K. A.; Kubiak, C. P. Recent Studies of Rhenium and Manganese Bipyridine Carbonyl Catalysts for the Electrochemical Reduction of CO_2. In *Advances in Inorganic Chemistry*; Aresta, M.; van Eldik, R., Eds.; Academic Press, 2014; Chapter 5, Vol. *66*, pp 163−188.

(8) Wang, J.-W.; Liu, W.-J.; Zhong, D.-C.; Lu, T.-B. Nickel complexes as molecular catalysts for water splitting and CO2 reduction. *Coord. Chem. Rev.* **2019**, *378*, 237−261.

(9) Boutin, E.; Merakeb, L.; Ma, B.; Boudy, B.; Wang, M.; Bonin, J.; Anxolabéhère-Mallart, E.; Robert, M. Molecular catalysis of CO2 reduction: recent advances and perspectives in electrochemical and light-driven processes with selected Fe, Ni and Co aza macrocyclic and polypyridine complexes. *Chem. Soc. Rev.* **2020**, *49*, 5772−5809.

(10) Rakowski Dubois, M.; Dubois, D. L. Development of Molecular Electrocatalysts for CO2 Reduction and H2 Production/Oxidation. *Acc. Chem. Res.* **2009**, *42*, 1974−1982.

(11) DuBois, D. L.; Miedaner, A.; Haltiwanger, R. C. Electrochemical reduction of carbon dioxide catalyzed by [Pd(triphosphine)(solvent)](BF4)2 complexes: synthetic and mechanistic studies. *J. Am. Chem. Soc.* **1991**, *113*, 8753−8764.

(12) Bernatis, P. R.; Miedaner, A.; Haltiwanger, R. C.; DuBois, D. L. Exclusion of Six-Coordinate Intermediates in the Electrochemical Reduction of CO2 Catalyzed by [Pd(triphosphine)(CH3CN)](BF4)-2 Complexes. *Organometallics* **1994**, *13*, 4835−4843.

(13) Miedaner, A.; Noll, B. C.; DuBois, D. L. Synthesis and Characterization of Palladium and Nickel Complexes with Positively Charged Triphosphine Ligands and Their Use as Electrochemical CO2-Reduction Catalysts. *Organometallics* **1997**, *16*, 5779−5791.

(14) Raebiger, J. W.; Turner, J. W.; Noll, B. C.; Curtis, C. J.; Miedaner, A.; Cox, B.; DuBois, D. L. Electrochemical Reduction of CO2 to CO Catalyzed by a Bimetallic Palladium Complex. *Organometallics* **2006**, *25*, 3345−3351.

(15) Therrien, J. A.; Wolf, M. O.; Patrick, B. O. Electrocatalytic Reduction of CO2 with Palladium Bis-N-heterocyclic Carbene Pincer Complexes. *Inorg. Chem.* **2014**, *53*, 12962−12972.

(16) Therrien, J. A.; Wolf, M. O.; Patrick, B. O. Polyannulated Bis(N-heterocyclic carbene)palladium Pincer Complexes for Electrocatalytic CO2 Reduction. *Inorg. Chem.* **2015**, *54*, 11721−11732.

(17) Therrien, J. A.; Wolf, M. O. The Influence of para Substituents in Bis(N-Heterocyclic Carbene) Palladium Pincer Complexes for Electrocatalytic CO2 Reduction. *Inorg. Chem.* **2017**, *56*, 1161−1172.

(18) Barlow, J. M.; Ziller, J. W.; Yang, J. Y. Inhibiting the Hydrogen Evolution Reaction (HER) with Proximal Cations: A Strategy for Promoting Selective Electrocatalytic Reduction. *ACS Catal.* **2021**, *11*, 8155−8164.

(19) Sinha, S.; Tran, G. N.; Na, H.; Mirica, L. M. Electrocatalytic H2 Evolution Promoted by a Bioinspired (N2S2)Ni(II) Complex. *Chem. Commun.* **2022**, *58*, 1143−1146.

(20) Chakrabarti, S.; Sinha, S.; Tran, G. N.; Na, H.; Mirica, L. M. Characterization of paramagnetic states in an organometallic nickel hydrogen evolution electrocatalyst. *Nat. Commun.* **2023**, *14*, No. 905.

(21) Chakrabarti, S.; Woods, T. J.; Mirica, L. M. *Insights into the Mechanism of CO2 Electroreduction by Molecular Palladium-Pyridinophane Complexes*; ChemRxiv, 2023 DOI: 10.26434/chemrxiv-2023-ds7dp (accessed Sept 04, 2023).

(22) Luo, J.; Tran, G. N.; Rath, N. P.; Mirica, L. M. Detection and Characterization of Mononuclear Pd(I) Complexes Supported by N2S2 and N4 Tetradentate Ligands. *Inorg. Chem.* **2020**, *59*, 15659−15669.

(23) Luo, J.; Khusnutdinova, J. R.; Rath, N. P.; Mirica, L. M. Unsupported d^8-d^8 Interactions in Cationic Pd^{II} and Pt^{II} Complexes:

Evidence for a Significant Metal-Metal Bonding Character. *Chem. Commun.* **2012**, *48*, 1532−1534.
(24) Tang, F.; Qu, F.; Khusnutdinova, J. R.; Rath, N. P.; Mirica, L. M. Structural and Reactivity Comparison of Analogous Organometallic Pd(III) and Pd(IV) Complexes. *Dalton Trans.* **2012**, *41*, 14046−14050.
(25) Luo, J.; Rath, N. P.; Mirica, L. M. Oxidative Reactivity of (N2S2)PdRX Complexes (R = Me, Cl; X = Me, Cl, Br): Involvement of Palladium(III) and Palladium(IV) Intermediates. *Organometallics* **2013**, *32*, 3343−3353.
(26) Khusnutdinova, J. R.; Luo, J.; Rath, N. P.; Mirica, L. M. Late First-Row Transition Metal Complexes of a Tetradentate Pyridinophane Ligand: Electronic Properties and Reactivity Implications. *Inorg. Chem.* **2013**, *52*, 3920−3932.
(27) Khusnutdinova, J. R.; Rath, N. P.; Mirica, L. M. The Conformational Flexibility of the Tetradentate Ligand tBuN4 is Essential for the Stabilization of (tBuN4)PdIII Complexes. *Inorg. Chem.* **2014**, *53*, 13112−13129.
(28) Sinha, S.; Mirica, L. M. Electrocatalytic O2 Reduction by an Organometallic Pd(III) Complex via a Binuclear Pd(III) Intermediate. *ACS Catal.* **2021**, *11*, 5202−5211.
(29) Savéant, J.-M.; Costentin, C. *Elements of Molecular and Biomolecular Electrochemistry: An Electrochemical Approach to Electron Transfer Chemistry*, 2nd ed.; John Wiley & Sons, Inc., 2019.
(30) Appel, A. M.; Helm, M. L. Determining the Overpotential for a Molecular Electrocatalyst. *ACS Catal.* **2014**, *4*, 630−633.
(31) Smieja, J. M.; Benson, E. E.; Kumar, B.; Grice, K. A.; Seu, C. S.; Miller, A. J. M.; Mayer, J. M.; Kubiak, C. P. Kinetic and structural studies, origins of selectivity, and interfacial charge transfer in the artificial photosynthesis of CO. *Proc. Natl. Acad. Sci. U.S.A.* **2012**, *109*, 15646−15650.
(32) Ragaini, F.; Larici, H.; Rimoldi, M.; Caselli, A.; Ferretti, F.; Macchi, P.; Casati, N. Mapping Palladium Reduction by Carbon Monoxide in a Catalytically Relevant System. A Novel Palladium(I) Dimer. *Organometallics* **2011**, *30*, 2385−2393.
(33) Ariyananda, P. W. G.; Yap, G. P. A.; Rosenthal, J. Reaction of carbon dioxide with a palladium−alkyl complex supported by a bis-NHC framework. *Dalton Trans.* **2012**, *41*, 7977−7983.
(34) Cecconi, F.; Ghilardi, C. A.; Midollini, S.; Moneti, S.; Orlandini, A.; Scapacci, G. Palladium complexes with the tripodal phosphine tris-(2-diphenylphosphinoethyl)amine. Synthesis and structure of trigonal, tetrahedral, trigonal bipyramidal, and square planar complexes. *J. Chem. Soc., Dalton Trans.* **1989**, 211−216.
(35) Mandal, S. K.; Sigman, M. S. Palladium-Catalyzed Aerobic Oxidative Kinetic Resolution of Alcohols with an Achiral Exogenous Base. *J. Org. Chem.* **2003**, *68*, 7535−7537.
(36) Yasuda, H.; Choi, J.-C.; Lee, S.-C.; Sakakura, T. Reactivity of Diaryloxy Palladium Complex with TMEDA (N,N,N′,N′-Tetramethylethylenediamine) Ligand toward Carbon Monoxide and Carbon Dioxide. *Organometallics* **2002**, *21*, 1216−1220.
(37) Pushkar, J.; Wendt, O. F. Reactivity of palladium(II) methyl complexes towards CO2: formation of carbonate complexes. *Inorg. Chim. Acta* **2004**, *357*, 1295−1298.

https://doi.org/10.1021/acs.inorgchem.3c02236
Inorg. Chem. 2023, 62, 16801−16809